Identification of chaperonin CCTγ subunit as a determinant of retinotectal development by whole-genome subtraction cloning from zebrafish *no tectal neuron* mutant

Naoto Matsuda and Masayoshi Mishina*

Department of Molecular Neurobiology and Pharmacology, Graduate School of Medicine, University of Tokyo, and SORST, Japan Science and Technology Agency, Tokyo 113-0033, Japan
*Author for correspondence (e-mail: mishina@m.u-tokyo.ac.jp)

Accepted 21 January 2004

Development 131, 1913-1925
Published by The Company of Biologists 2004
doi:10.1242/dev.01085

Summary

Zebrafish *no tectal neuron* (*ntn*) mutant obtained by trimethylpsoralen (TMP) mutagenesis showed defects in tectal neuropil formation and small eyes. We carried out whole-genome subtraction between wild-type and mutant zebrafish embryos using the representational difference analysis (RDA) method. Nineteen subtraction products enabled us to construct genetic and physical maps of the *ntn* region. Direct selection of cDNAs using a YAC clone encompassing the *ntn* locus and RT-PCR analysis of transcripts identified a 143 bp deletion in the *cct3* gene encoding the γ subunit of chaperonin containing TCP-1 (CCT). Injection of antisense *cct3* morpholino oligonucleotides into zebrafish embryos induced characteristic *ntn* phenotypes including defects in retinal ganglion cell (RGC) differentiation and tectal neuropil formation. Moreover, injection of *cct3* mRNA successfully rescued *ntn* mutant embryos. Our results suggest that RDA is an efficient and widely applicable cloning strategy in zebrafish genetics. The strong expression of the *cct3* mRNA started in the entire embryos by 12 hpf and was sustained thereafter, but there were no detectable abnormalities in body patterning and neurogenesis in *ntn* mutant embryos at 30 hpf. The expression patterns of transcription factor genes *ath5* and *brn3b* that are essential for the development and maintenance of RGCs were indistinguishable between wild-type and *ntn* mutant embryos, but those of early and late differentiation markers of RGCs, nicotinic acetylcholine receptor β3 and zn5, were diminished in mutant embryos. Immunostaining of acetylated tubulin also revealed the impairment of RGC neurite extension. Thus, the *ntn* mutation of the *cct3* gene impaired the differentiation of retinal neuroepithelial cells to RGCs. Similarly, the expression of *brn3b* was normal in the tectum of *ntn* mutants, but tectal neuropil formation was abolished. These results suggest that the γ subunit of chaperonin CCT plays an essential role in retinotectal development.

Key words: Zebrafish, Trimethylpsoralen (TMP) mutagenesis, Representational difference analysis (RDA), Chaperonin containing TCP-1 γ subunit (CCTγ), Retinotectal development

Introduction

Zebrafish (*Danio rerio*) is an excellent model organism with which to investigate gene function in vertebrates because external fertilization, transparent embryos and random mutagenesis techniques facilitate phenotype-driven forward genetic analyses (Eisen, 1996). Large-scale screening of zebrafish mutagenized by *N*-ethyl-*N*-nitrosourea (ENU) identified ~2400 mutations affecting development and behavior (Driever et al., 1996; Haffter et al., 1996). However, molecular cloning of ENU-induced mutant genes will require positional cloning and/or candidate gene approaches (Postlethwait and Talbot, 1997), because ENU induces predominantly substitution mutations (Mullins et al., 1994; Solnica-Krezel et al., 1994). Thus, availability of polymorphic markers will be rate-limiting. In terms of cloning, insertion mutagenesis with pseudotype retroviruses is a straightforward approach to obtain mutated genes (Gaiano et al., 1996). Hopkins and colleagues isolated more than 500 insertional mutants (Golling et al., 2002), but the efficiency of mutagenesis was lower than ENU mutagenesis (Amsterdam et al., 1999).

To investigate the molecular mechanisms underlying neural network formation, we developed a highly efficient mutagenesis procedure using 4,5′,8-trimethylpsoralen (TMP) (Ando and Mishina, 1998). In a pilot screen, we isolated and characterized two mutant lines with abnormalities in the nervous system. The *no tectal neuron* (*ntn*) mutation impaired the development of tectal neurons and eyes, whereas the *edawakare* mutation affected the arborization of the trigeminal ganglion and Rohon-Beard sensory neurons. TMP is a DNA crosslinking agent that can frequently induce small deletions in combination with UV irradiation in *Escherichia coli* and *Caenorhabditis elegans* (Sladek et al., 1989; Yandell et al., 1994; Liu et al., 1999). A potential advantage of the method would be that one could isolate mutagenized genes directly by whole-genome subtraction using TMP-induced deletions as molecular tags. Representational difference analysis (RDA) is a powerful subtraction method of the entire genome (Lisitsyn and Wigler, 1993).

We have applied RDA to characterize the genomic region of the TMP-induced *ntn* mutation (Ando and Mishina, 1998). Successful isolation of tightly linked polymorphic markers by the whole-genome subtraction method led to the construction of genetic and physical maps of the zebrafish genomic region responsible for retinotectal development. RT-PCR analysis of transcripts from the *ntn* region identified a 143 bp deletion in the *cct3* gene encoding the γ subunit of chaperonin containing TCP1 (CCT, also called the TCP1 ring complex or TriC). Injection of antisense *cct3* morpholino oligonucleotides into zebrafish embryos induced characteristic *ntn* phenotypes, including the degeneration of retinal ganglion cells and tectal neurons. Furthermore, injection of *cct3* mRNA successfully rescued *ntn* mutant embryos. These results revealed that chaperonin CCTγ controls specifically retinotectal development in zebrafish. Our results open a novel TMP mutagenesis-RDA cloning strategy of zebrafish forward genetics characterized by high efficiency and rapid cloning.

Materials and methods

Strains and breeding of zebrafish

Zebrafish of the AB strain were raised and kept under standard conditions at ~28°C (Mullins et al., 1994). The *ntn* mutant line *jt5* was isolated by TMP mutagenesis previously (Ando and Mishina, 1998). The *ntn* mutant embryos at 3 days postfertilization (dpf) showed small eyes and turbid tectum. Mutation carriers were identified by random intercrosses and were then outcrossed to wild-type zebrafish of the AB strain. Mutant embryos were obtained by crossing heterozygous fish. The transgenic zebrafish line carrying the nicotinic acetylcholine receptor β3 (nAChRβ3) gene promoter-driven enhanced green fluorescent protein (EGFP) expression vector (PAR-EGFP) has been established previously (Tokuoka et al., 2002). Embryos were raised at 28.5°C in embryo rearing solution (ERS) (Easter and Nicola, 1996). For microscopic observation, 0.2 mM phenylthiocarbamide was added to ERS at 12 hours postfertilization (hpf) to prevent melanocyte pigmentation (Westerfield, 1995).

RDA procedure

Genomic DNAs were prepared from pools of 40 mutant embryos and 40 wild-type siblings and RDA was performed essentially as described (Lisitsyn et al., 1994; Lisitsyn and Wigler, 1995). Genomic DNAs (1 μg of each) were digested with *Bgl*II, *Eco*RI, *Hin*dIII, *Spe*I and *Xba*I, and were PCR-amplified to generate amplicons. Primer sequences were designed according to the protocol (Lisitsyn and Wigler, 1995) with some modifications on their cohesive end sequences compatible for the restriction endonuclease (Table 1). The iterative hybridization-amplification step was repeated three times for *Bgl*II, *Eco*RI, *Spe*I or *Xba*I amplicons and four times for *Hin*dIII amplicons. The resulting RDA products were digested with the corresponding restriction enzymes, agarose gel-isolated and cloned into pBluescript II SK(+) (Stratagene). Genomic DNA with respective restriction enzymes and amplicon (5 μg of each) were electrophoresed in 2% agarose gels and transferred to Hybond-N^+ nylon membranes (Amersham). Membranes were hybridized with RDA products labeled using a random primed DNA labeling kit (Roche) as probes.

Genetic mapping

Genomic DNA was extracted from 93 pools of five *ntn* mutant embryos obtained from crosses of heterozygous fish. One μg genomic DNA from each pool was digested with *Bgl*II, *Eco*RI, *Hin*dIII, *Spe*I or *Xba*I. Digested DNAs were PCR-amplified to generate amplicons as above. Southern hybridization analyses of amplicons with RDA products were performed.

Genomic sequences flanking the restriction fragment length polymorphism (RFLP) sites of RDAjt5B430, RDAjt5B460 and RDAjt5E340 were cloned by vectorette-PCR using a GenomeWalker kit (Clontech), and primers were designed to identify cleaved amplified polymorphic sequences (CAPS): RDAjt5B430 RFLP site, 5′-TGGCGGTTCATTCTGCTGTGCGAC-3′ and 5′-CGACAAGAC-TTTTGTCAGGTAG-3′; RDAjt5B460 RFLP site, 5′-CAATACC-GGCAACTTTCAAC-3′ and 5′-CAAGGACAAGAAATCATGCC-3′; and RDAjt5E340 RFLP site, 5′-GTCAAAATGCTCACTATA-CTAACTGCTGTC-3′ and 5′-AGTTTCGGCTTGGTTACGGAA-TCTC-3′. Mapping of YD1 and YH2 loci was carried out by PCRs using primers flanking the deletions; YD1 locus, 5′-GACA-GTGGAAATGCGGCTAT-3′ and 5′-TACCCATGTCTTCTGC-GTAG-3′; YH2 locus, 5′-GGCCAGAGTTTACATAGGGGT-3′ and 5′-GGTTTTTGCTGTGTCTGCCTG-3′. Radiation hybrid (RH) mapping was performed on the Goodfellow zebrafish T51 RH panel (Research Genetics) (Geisler et al., 1999) using the primers for the RDAjt5E340 RFLP site and YD1 locus.

Table 1. Primers for RDA

Enzyme	Name	Sequence
*Bgl*IIR	Bgl24	5′-AGCACTCTCCAGCCTCTCACCGCA-3′
	R Bgl12	5′-GATCTGCGGTGA-3′
	J Bgl24	5′-ACCGACGTCGACTATCCATGAACA-3′
	J Bgl12	5′-GATCTGTTCATG-3′
	N Bgl24	5′-AGGCAACTGTGCTATCCGAGGGAA-3′
	N Bgl12	5′-GATCTTCCCTCG-3′
*Eco*RI	R Eco24	5′-AGCACTCTCCAGCCTCTCACCGAG-3′
	R Eco12	5′-AATTCTCGGTGA-3′
	J Eco24	5′-ACCGACGTCGACTATCCATGAACG-3′
	J Eco12	5′-AATTCGTTCATG-3′
	N Eco24	5′-AGGCAACTGTGCTATCCGAGGGAG-3′
	N Eco12	5′-AATTCTCCCTCG-3′
*Hin*dIII	R Hind24	5′-AGCACTCTCCAGCCTCTCACCGCA-3′
	R Hind12	5′-AGCTTGCGGTGA-3′
	J Hind24	5′-ACCGACGTCGACTATCCATGAACA-3′
	J Hind12	5′-AGCTTGTTCATG-3′
	N Hind24	5′-AGGCAGCTGTGGTATCGAGGGAGA-3′
	N Hind12	5′-AGCTTCTCCCTC-3′
*Spe*I	R Spe24	5′-AGCACTCTCCAGCCTCTCACCGCA-3′
	R Spe12	5′-CTAGTGCGGTGA-3′
	J Spe24	5′-ACCGACGTCGACTATCCATGAACA-3′
	J Spe12	5′-CTAGTGTTCATG-3′
	N Spe24	5′-AGGCAGCTGTGGTATCGAGGGAGA-3′
	N Spe12	5′-CTAGTCTCCCTC-3′
*Xba*I	R Xba24	5′-AGCACTCTCCAGCCTCTCACCGTT-3′
	R Xba12	5′-CTAGAACGGTGA-3′
	J Xba24	5′-ACCGACGTCGACTATCCATGAACT-3′
	J Xba12	5′-CTAGAGTTCATG-3′
	N Xba24	5′-AGGCAGCTGTGGTATCGAGGGAGT-3′
	N Xba12	5′-CTAGACTCCCTC-3′

Genomic DNA library screening and cDNA cloning

YAC clones D04128 and H0145 were obtained by PCR screening of a zebrafish YAC library (Resource Center/Primary Databank, Germany) with the primers for RDAjt5E340 RFLP site and their terminal sequences were determined as described (Zhong et al., 1998). PAC 10J03 and BAC 18M9 clones were isolated from zebrafish BAC and PAC libraries (Genome Systems) using ^{32}P-labeled RDAjt5B430 and RDAjt5E340 as probes, respectively. The inserts of these clones were sized by pulsed-field gel electrophoresis using CHEF-Mapper (BioRad). For YAC clonality analysis, the blot was probed with the ^{32}P-labeled YAC arm pRML plasmid.

Zebrafish genomic DNA in YAC D04128 clone purified by pulsed-field gel electrophoresis was biotinylated using a random primed DNA labeling kit (Roche). A random primed zebrafish cDNA library was synthesized using RNA from zebrafish embryos at 36 hpf as templates (SuperScript Choice System, Invitrogen) and PCR-amplified after

ligation to adapters 5′-TAGTCCGAATTCAAGCAAGAGCAGA-3′ and 5′-CTCTTGCTTGAATCGGACTA-3′. After preincubation with 2 μg sonicated zebrafish genomic DNA and 1 μg *Hae*III-digested yeast genomic DNA, 1 μg preamplified cDNA was hybridized with 100 ng biotinylated zebrafish genomic DNA in YAC D04128 clone as described (Del Mastro and Lovett, 1996). The sequences of the 5′ and 3′ regions of the *cct3* cDNA were obtained by 5′- and 3′-rapid amplification of cDNA ends (RACE) using a SMART cDNA kit (Clontech), respectively. The entire coding sequence of *cct3* cDNA was cloned into pCRII vector (Invitrogen) by RT-PCR with primers, 5′-TGTCCGGTACCGGTGATCTAAC-3′ and 5′-AAATGGATTT-CTGATGAGAACGTTGT-3′ to yield pCRII-CCT3. The deletion mutation in the *cct3* mRNA was identified by sequencing RT-PCR products of mRNAs from ~200 *ntn* homozygous embryos and ~650 wild-type siblings at 50 hpf according to the protocol of the SuperScript Choice System (Invitrogen). The mutation in the *cct3* gene was confirmed by PCR on 100 ng genomic DNAs from ~300 wild-type siblings and ~100 *ntn* embryos with primers flanking the 143 bp deletion, 5′-GCCATGCAAGTGTGTCGTAATG-3′ and 5′-CTCAGAGAAGTGAGCACACGAATG-3′. Genotyping of embryos was performed using the same primer set.

In situ hybridization

The entire coding sequence of the zebrafish *brn3b/pou4f1* was obtained by RT-PCR using primers 5′-CGGTCGCAAATATGA-TGATG-3′ and 5′-ATGATTCCACATCCCCTTTG-3′, and was cloned into pCRII vector to yield pCRII-BRN3B (GenBank Accession Number AB122025). We carried out whole-mount in situ hybridization with antisense RNA probes prepared with a DIG RNA labeling kit (Roche), paraffin-embedding and sectioning of whole embryos as described previously (Mori et al., 1994; Jowett, 1999). Deparaffinized sections were counterstained with 0.5% Methyl Green for 10 minutes. Probes for *ath5/lakritz*, *dlx2*, *hlx1*, *krox20*, *myod*, *ntl*, *pax2a/noi* (previously *pax2.1*), *shh* and *zash1* mRNAs were as described previously (Masai et al., 2000; Akimenko et al., 1994; Seo et al., 1999; Oxtoby and Jowett, 1993; Weinberg et al., 1996; Schulte-Merker et al., 1994; Krauss et al., 1991; Krauss et al., 1993; Allende and Weinberg, 1994).

Stainings

Whole-mount immunostaining of zebrafish embryos with anti-acetylated tubulin antibody (Sigma) were carried out as previously described (Hammerschmidt et al., 1996) except that Alexa 488 anti-mouse IgG antibody was used as secondary antibody. Immunostaining of cryosectioned embryos using a monoclonal antibody zn5 (Oregon Monoclonal Bank) was performed as described (Masai et al., 2003). Terminal deoxynucleotide transferase-mediated dUTP nick-end labeling (TUNEL) was carried out in cryosections according to the manufacturer's protocol (ApopTag Apoptosis Detection Kit; Serologicals Corporation).

Dechorionated embryos were soaked in ERS containing 5 μg/ml Acridine Orange (Sigma) or 100 μM Bodipy-ceramide (Fl C5, Molecular Probes) and 2% DMSO for 30 minutes in the dark. The embryos were washed, anesthetized by 0.02% 3-aminobenzoic acid ethyl ester (tricaine, Sigma) and embedded in low-melting temperature agarose gels during microscopic observation. The eyes and tectum of Bodipy-ceramide-stained embryos were scanned by confocal microscopy.

Phenocopy by antisense morpholino oligonucleotides and phenotypic rescue by RNA injections

The fluorescein-tagged morpholino oligonucleotide complementary to the nucleotide residues –16 to +9 of the zebrafish *cct3* mRNA (nucleotide residues are numbered from the putative translational initiation codon, GenBank Accession Number AF506209) (Golling et al., 2002) was obtained from GeneTools. The antisense or control oligonucleotide at a concentration of 4 μg/μl in 1× Danieau buffer (Nasevicius and Ekker, 2000) was injected into the yolk of one- to four-cell stage wild-type or transgenic embryos carrying PAR-EGFP using a microinjector (IM-300, Narishige). Distribution of oligonucleotides in embryos was monitored under fluorescent microscopy. Fluorescence of EGFP was much stronger and easily distinguishable from that of fluorescein. Fluorescence of EGFP-labeled retinal ganglion cell (RGC) axons was observed as described (Tokuoka et al., 2002).

The 1.8 kb *Eco*RV-*Spe*I fragment from pCRII-CCT3 was cloned into the *Stu*I and *Xba*I sites of pCS2+ vector (Turner and Weintraub, 1994) to yield pCS-CCT3. Capped *cct3* mRNA was prepared from 1 μg pCS-CCT3 linearized with *Not*I using an mMessage mMachine kit (Ambion). We injected 110-270 pg mRNA into the cytoplasm of embryos produced by crossing heterozygous fish.

Results

Localization of *ntn* mutant locus by whole-genome subtraction

Zebrafish *no tectal neuron* (*ntn*) mutants isolated by TMP mutagenesis showed degeneration of tectal neurons and eyes (Ando and Mishina, 1998). The ntn^{jt5} allele was of recessive inheritance and fully penetrant. If TMP mutagenesis induces deletions in the zebrafish genome as in *E. coli* and *C. elegans* (Sladek et al., 1989; Yandell et al., 1994; Liu et al., 1999), it would be possible to directly clone deleted DNA segments by subtraction between pooled wild-type and mutant genomes. Alternatively, such whole-genome subtraction may allow us to obtain DNA segments tightly linked to the *ntn* locus if there were enough RFLPs in the AB strain genome. We subtracted the mutant genome from the wild-type sibling genome by the RDA method (Lisitsyn and Wigler, 1993). Zebrafish genomic DNA was digested with various 6 bp recognizing restriction endonucleases, and five enzymes that produced DNA fragments with short mean lengths appropriate for RDA were selected. We prepared PCR-amplified DNA fragments (amplicons) of genomic DNA from pools of 40 *ntn* mutant embryos and 40 wild-type siblings using each of *Bgl*II, *Eco*RI, *Hin*dIII, *Spe*I and *Xba*I restriction enzymes. Whole-genome subtraction was carried out using the amplicons from the wild-type genome as the tester and those from the *ntn* mutants as the driver. After three or four rounds of the subtractive hybridization amplification, difference products became detectable as clearly seen bands in agarose gels from respective amplicons (Fig. 1A). We thus successfully obtained six RDA products from the *Bgl*II amplicons designated as RDAjt5B430 (B430), RDAjt5B440 (B440), RDAjt5B460 (B460), RDAjt5B470 (B470), RDAjt5B610 (B610) and RDAjt5B630 (B630); five products from the *Eco*RI amplicons designated as RDAjt5E230 (E230), RDAjt5E340 (E340), RDAjt5E420 (E420), RDAjt5E550 (E550) and RDAjt5E560 (E560); two products from *Hin*dIII amplicons designated as RDAjt5H400 (H400) and RDAjt5H480 (H480); one product from the *Spe*I amplicons designated as RDAjt5S610 (S610); and five products from the *Xba*I amplicons designated as RDAjt5X300 (X300), RDAjt5X350 (X350), RDAjt5X430 (X430), RDAjt5X520 (X520) and RDAjt5X600 (X600). Southern blot hybridization analysis of genomic DNA from *ntn* mutants and wild-type siblings showed that each RDA product hybridized with two fragments in the wild-type genome, but with only the larger one in the mutant genome digested by the corresponding restriction enzymes (Fig. 1B). Two hybridizing fragments were

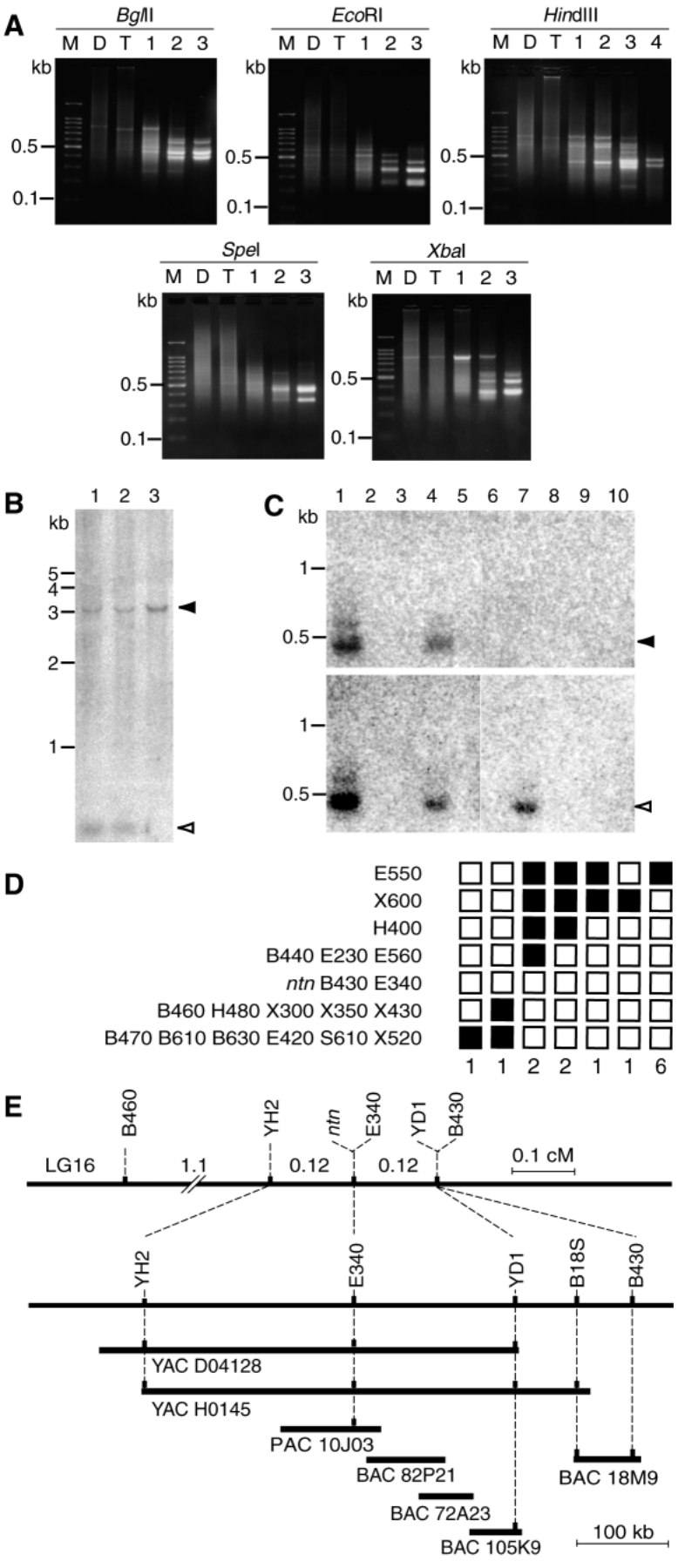

Fig. 1. Whole-genome subtraction between *ntn* mutant embryos and wild-type siblings by RDA. (A) Analysis of RDA products by agarose gel electrophoresis. Driver and tester amplicons were prepared by digestion of genomic DNA from wild-type and *ntn* mutant embryos using *Bgl*II, *Eco*RI, *Hin*dIII, *Spe*I and *Xba*I restriction endonucleases, respectively. Lane M, 100 bp DNA ladder as size markers; lane D, driver amplicons; lane T, tester amplicons; lanes 1-4, RDA products of the first, second, third and fourth rounds of subtraction, respectively. (B) Southern blot hybridization analysis of genomic DNA using RDA product E340 as a probe. Genomic DNAs from a wild-type fish of AB strain (lane 1), wild-type siblings (lane 2) and *ntn* mutant embryos (lane 3) were digested with *Eco*RI and hybridized to E340 probe. The sizes of markers in kb are indicated on the left. Black and white arrowheads on the right indicate the 3.1 kb and 0.3 kb *Eco*RI-digested DNA fragments representing polymorphic alleles, respectively. (C) An example of amplicon Southern blot hybridization analysis. Amplicons were prepared from *Bgl*II-digested genomic DNA from pools of five wild-type (lane 1) or *ntn* mutant (lanes 2-10) embryos. Blots were hybridized to B460 (upper) or B470 (lower) probe. Black and white arrowheads indicate fragments in the amplicons hybridizing to B460 and B470 probes, respectively. (D) Amplicon Southern hybridization mapping of the *ntn* locus using polymorphic RDA products. Amplicons prepared from 93 pools of five *ntn* mutant embryos were hybridized to respective RDA products. Black and white boxes indicate the presence and absence of amplicons hybridizing to RDA products, respectively. The numbers of pools containing recombinant(s) are given below. (E) Genetic and physical maps of the zebrafish *ntn* region on the linkage group 16. Numbers in the genetic map (upper) indicate genetic distances in cM between the markers. Physical map around the *ntn* locus is shown below with markers. Distances in the map are approximately to scale. Short horizontal lines below the physical map indicate YAC, PAC and BAC clones. BAC clones, 82P21, 72A23 and 105K9, were isolated by screening with C18orf1-like cDNAs as probes. B18S is a marker derived from the Sp6 end of BAC 18M9.

also present in the genome of the AB strain. These results suggest that all the RDA products resulted from RFLPs between the wild-type and *ntn* mutant genomes, rather than deletions in the mutant genome. We thus obtained polymorphic markers linked to the *ntn* locus by genetically directed RDA.

We then genetically selected polymorphic markers close to the *ntn* locus by Southern blot hybridization analysis of amplicons prepared from genomic DNA of 465 *ntn* mutant embryos. Genomic DNAs isolated from 93 pools of five mutant embryos were digested with the five restriction endonucleases used for RDA and amplicons were prepared. Blots of 93 amplicons were hybridized with the RDA products (Fig. 1C). The numbers of hybridization positive amplicons in the 93 amplicons were one for B460, H480, X300, X350 and X430; two for B440, B470, B610, B630, E230, E420, E560, S610 and X520; four for H400; six for X600; and eleven for E550. The genotyping of 93 mutant embryo pools revealed the positions of the polymorphic markers relative to the *ntn* locus (Fig.

1D). No recombinants among the *ntn*, B430 and E340 loci were found in 465 mutant embryos. The genetic mapping localized the *ntn* locus between the B440/E230/E560 and B460/H480/X300/X350/X430 loci.

We further determined the genotypes of 432 *ntn* mutant embryos for the B430 and E340 loci using CAPS markers. There was one recombination event between the *ntn* and B430 loci, the calculated genetic distance being 0.12 cM (95% confidence interval, 0.00-0.64 cM). However, we found no recombination events between the *ntn* and E340 loci. Thus, among isolated polymorphic RDA markers, E340 was the marker closest to the *ntn* locus.

We next screened zebrafish genomic libraries with E340 as a probe and obtained two YAC clones and one PAC clone (Fig. 1E). YAC H0145 contained a terminal sequence of BAC clone 18M9 obtained by screening with B430 as a probe. By comparing the 2.4 kb terminal sequences of YAC D04128 and the 2.9 kb terminal sequences of YAC H0145 with the corresponding genomic sequences of wild-type and *ntn* mutant embryos, we found 28 bp and 107 bp deletions in the *ntn* genome, designated as YD1 and YH2, respectively (Fig. 1E). Genotyping of 432 *ntn* mutant embryos by PCR using primers flanking the deletions in respective YAC ends identified one recombination event out of 864 meioses between the *ntn* and YH2 loci and one between the *ntn* and YD1 loci. We detected ten recombinations between the *ntn* and B460 loci by genotyping 432 *ntn* mutants using B460 CAPS marker. Thus, the relative order of markers around the *ntn* locus on the chromosome was B460-YH2-*ntn*/E340-YD1-B430 (Fig. 1E). These analyses localized the *ntn* locus within a 0.24 cM region between YH2 and YD1 markers.

Transcripts from the *ntn* region

Using YAC D04128 as a probe, we isolated ~300 cDNA clones by screening a cDNA library prepared from zebrafish embryos at 36 hpf. Sequence analysis suggested that these clones encoded at least three genes. The first group of 26 cDNA clones and zebrafish ESTs (EST269466, fb13f04, fc26d03, fc72f03 and fe18d09) from the database of the Washington University zebrafish EST project encoded the γ subunit of zebrafish chaperonin CCT, which shared 87%, 86%, 85%, 70% and 58% amino acid sequence identities with the *Xenopus laevis*, mouse, human, *Drosophila melanogaster* and yeast counterparts, respectively (Chen et al., 1994; Kubota et al., 1994; Dunn and Mercola, 1996; Walkley et al., 1996a; Walkley et al., 1996b; Walkley and Malik, 1996). The second group of five cDNA clones encoded a putative protein that had 69% amino acid sequence identity with human C18orf1, a transmembrane protein with a LDL receptor type A domain (Yoshikawa et al., 1998). A putative protein encoded by the third group of seven cDNAs showed 32% amino acid sequence identity with mouse semaphorin 6C precursor (Kikuchi et al., 1999). One cDNA contained a single open reading frame, but there found no proteins homologous to the putative protein. The rest of the cDNA clones contained (CA)n dinucleotide repetitive sequences of various length and were not characterized further.

By RT-PCR analysis of mRNAs, we found a 143 bp deletion in the CCT γ subunit gene (*cct3*) transcript from the mutant embryos (Fig. 2A,B). The deletion was present in the *cct3* gene of mutant embryos, but not in the wild-type gene (Fig. 2C). The γ subunit of zebrafish CCT consisted of 543 amino acids and had five regions common to the CCT subunit proteins (Kim et al., 1994), the N- and C-terminal equatorial ATPase domains, two intermediate domains and the apical substrate-binding domain (Fig. 2A). The *cct3* transcript in the mutant embryos completely lacked a putative ATPase motif and the reading frame was shifted by the deletion. There were no mutations within the coding sequences of three other candidate gene transcripts.

We studied the expression of the *cct3* gene by in situ hybridization analysis (Fig. 2D). No transcripts were detectable in one-cell, shield and 90% epiboly stage embryos at 0.2, 6 and 9 hpf. At 12 hpf, strong hybridization signals for the *cct3* mRNA appeared in the entire embryos. The *cct3* mRNA was detected throughout the body at 24 hpf, and the brain, eyes and somites showed strong hybridization signals. At 36 hpf, hybridization signals for the *cct3* mRNA were observed in the entire brain and somites.

Identification of the *ntn* mutant gene

The characteristic phenotypes of *ntn* mutant embryos were selective impairment of development of the eyes and tectum at ~40 hpf (Ando and Mishina, 1998). At later stages (4 dpf), *ntn* mutants can be macroscopically distinguished from their wild-type siblings as having small eyes and turbidity in the developing tectum (Fig. 3A). There appeared no other abnormalities even at this stage except for small pectoral fins and some underdeveloped jaw skeletons in *ntn* mutant embryos.

At 36 hpf, Acridine Orange staining (Abrams et al., 1993; Furutani-Seiki et al., 1996) showed strong signals selectively in the tectum of mutant embryos, suggesting apoptotic cell death (Fig. 3B). In fact, staining with Bodipy-ceramide, which was freely distributed in the interstitium between cells and delineated cellular membrane (Cooper et al., 1999), revealed patches of cell-free space probably reminiscent of engulfed dead cells in the tectum of mutant embryos at 46 hpf (Fig. 3C). Furthermore, the tectum of the mutant embryos at 48 hpf was hardly stained by antibody against acetylated tubulin (Fig. 3D), a marker protein of mature neurites (Chitnis and Kuwada, 1990), as described previously (Ando and Mishina, 1998). Neurites in the retinal ganglion cell layer were poorly developed and the bundle of the optic nerve was faint in *ntn* mutants (Fig. 3E). However, the staining patterns of other neurons such as axons of the anterior commissure neurons, hindbrain neurons, trigeminal ganglion cells and dorsal longitudinal fascicles were comparable between wild-type and mutant embryos (Fig. 3D,E).

To examine whether the mutation in the *cct3* gene was responsible for the *ntn* phenotypes, we injected an antisense morpholino oligonucleotide complementary to the *cct3* mRNA sequence encompassing the translation start codon into the wild-type embryos. The injected embryos showed small eyes at 4 dpf (Fig. 3F) and Acridine Orange staining in the tectum at 36 hpf (Fig. 3G). Bodipy-ceramide staining revealed loss of tectal cells (Fig. 3H). Anti-acetylated tubulin antibody immunostaining demonstrated that the formation of tectal neuropil and optic nerve was impaired in the embryos injected with an antisense morpholino oligonucleotide (Fig. 3I,J). Injection of a control morpholino oligonucleotide with the inverted antisense sequence exerted little effect on the development of the tectal and retinal neurons (Fig. 3F-J). These

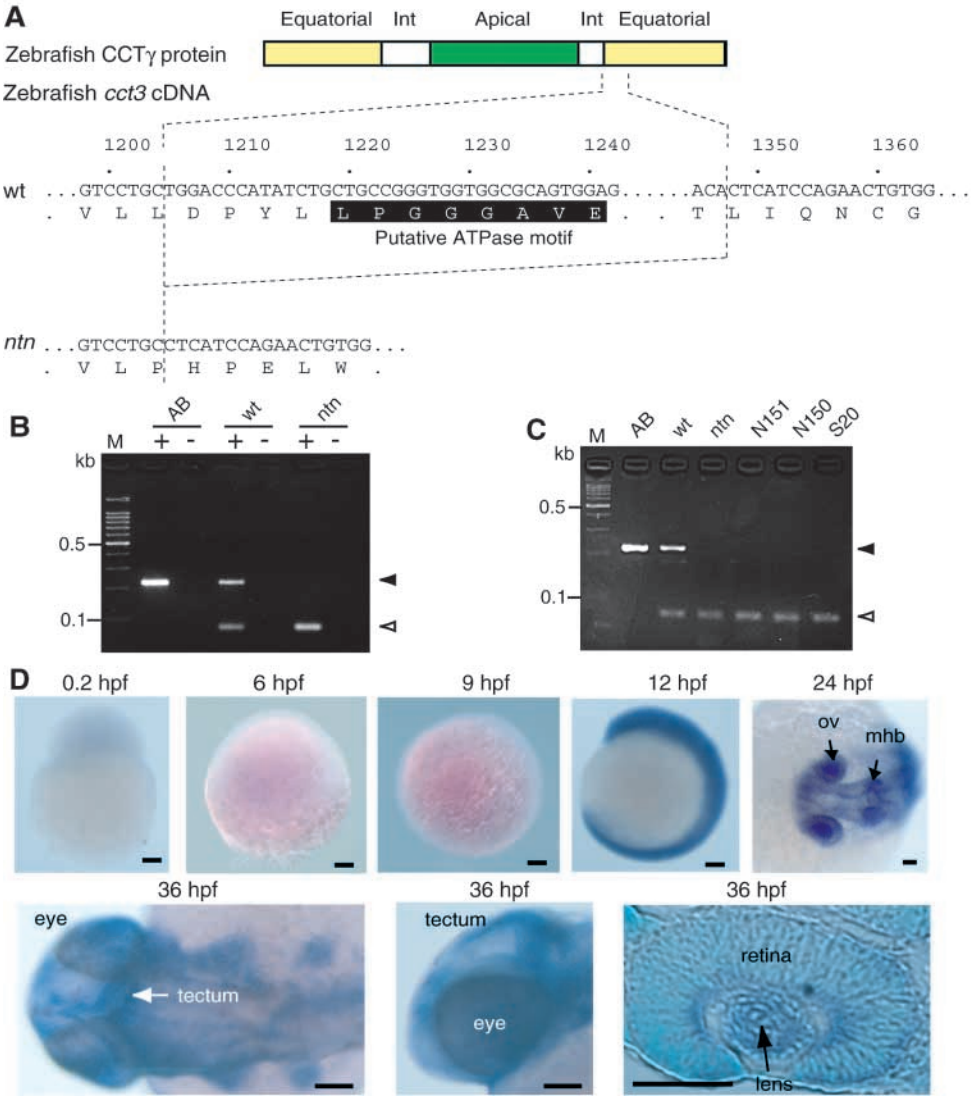

Fig. 2. Identification of an internal deletion in the *ntn* mutant *cct3* gene and expression of the *cct3* mRNA in wild-type embryos during development. (A) A 143 bp internal deletion in the *cct3* transcript. The zebrafish CCT γ subunit is schematically shown above; the equatorial, apical and intermediate regions are indicated in boxes. The nucleotide sequences of a putative ATPase motif in the wild-type (wt) and mutant (*ntn*) *cct3* transcripts are shown below. The 143 bp deletion corresponding to the nucleotide residues 1205-1347 of the zebrafish *cct3* transcript is in the coding sequence for a putative ATPase motif of CCTγ. The deletion causes frame-shift and aberrant termination of translation. (B) RT-PCR analysis of the *cct3* gene transcripts from pools of ~1190 wild-type embryos of the AB strain (AB), ~650 wild-type siblings (wt) and ~200 mutant (*ntn*) embryos with (+) or without (–) a reverse transcriptase using primers flanking the 143 bp deletion. Lane M shows 100 bp DNA ladder as size markers. Black and white arrowheads on the right indicate the 221 bp and 78 bp PCR products representing intact and deleted transcripts, respectively. (C) PCR analysis of genomic DNA from pools of ~100 wild-type embryos of AB strain (AB), ~300 wild-type siblings (wt), ~100 mutant (*ntn*) and three individual mutant (N151, N150 and S20) embryos using primers flanking the 143 bp deletion. Lane M shows 100 bp DNA ladder as size markers. Black and white arrowheads on the right indicate the 221 bp and 78 bp PCR products representing the intact and deleted *cct3* genes, respectively. (D) Whole-mount in situ hybridization analysis of *cct3* mRNA at 0.2 hpf (one-cell stage), 6 hpf (shield stage), 9 hpf (90%-epiboly stage), 12 hpf, 24 hpf and 36 hpf. A section through the retina was shown for embryos at 36 hpf. mhb, midbrain-hindbrain boundary; ov, optic vesicle. Scale bars: 100 μm.

results suggest that suppression of CCTγ expression by the antisense morpholino oligonucleotide induces the characteristic phenotypes of *ntn* mutant embryos.

We next injected wild-type *cct3* mRNA into one-cell stage embryos derived from crosses of heterozygous (+/–) fish to examine whether the *cct3* gene could rescue *ntn* mutant embryos. The injected embryos were stained with Acridine Orange for testing the *ntn* mutant phenotypes (Fig. 3K). Among 77 embryos injected with *cct3* mRNA, only four embryos (5%) showed strong Acridine Orange staining in the tectum at 36 hpf and 73 embryos (95%) appeared normal, which deviated significantly from recessive inheritance (χ^2 test, P<0.001). The genotyping of embryos with wild-type phenotypes revealed that 11 of 73 embryos were *cct3*$^{-/-}$ at the *ntn* locus. The genotype at the *ntn* locus of 20 embryos was *cct3*$^{+/+}$ and that of remaining 42 embryos was *cct3*$^{+/-}$. Among 137 mock-injected embryos, 37 embryos (27%) showed the *ntn* mutant phenotypes (Fig. 3K) and 100 embryos (73%) exhibited the wild-type phenotypes, which was consistent with a recessive mode of inheritance (χ^2 test, P=0.70). In 100 mock-injected embryos showing wild-type phenotypes, there were no embryos with *cct3*$^{-/-}$ genotype at the *ntn* locus. All the embryos with wild-type phenotypes had genotypes of either *cct3*$^{+/+}$ or *cct3*$^{+/-}$ at the *ntn* locus. The development of the eyes at 3 dpf was normal in the embryos that did not show an increase in Acridine Orange staining in the tectum. These results suggest that injection of *cct3* mRNA rescued *ntn* mutant embryos.

The gene encoding nAChRβ3 is an early differentiation marker of RGCs (Matter-Sadzinski et al., 2001). To examine the differentiation of RGCs, we crossed the heterozygous *ntn* fish with a transgenic zebrafish carrying the nAChRβ3 gene promoter-directed EGFP expression vector (Tokuoka et al., 2002). Crossing of doubly transgenic fish with heterozygous *ntn* fish yielded homozygous mutant embryos with EGFP-labeled RGCs. Expression of EGFP signals in *ntn* embryos injected with *cct3* mRNA indicated the restoration of

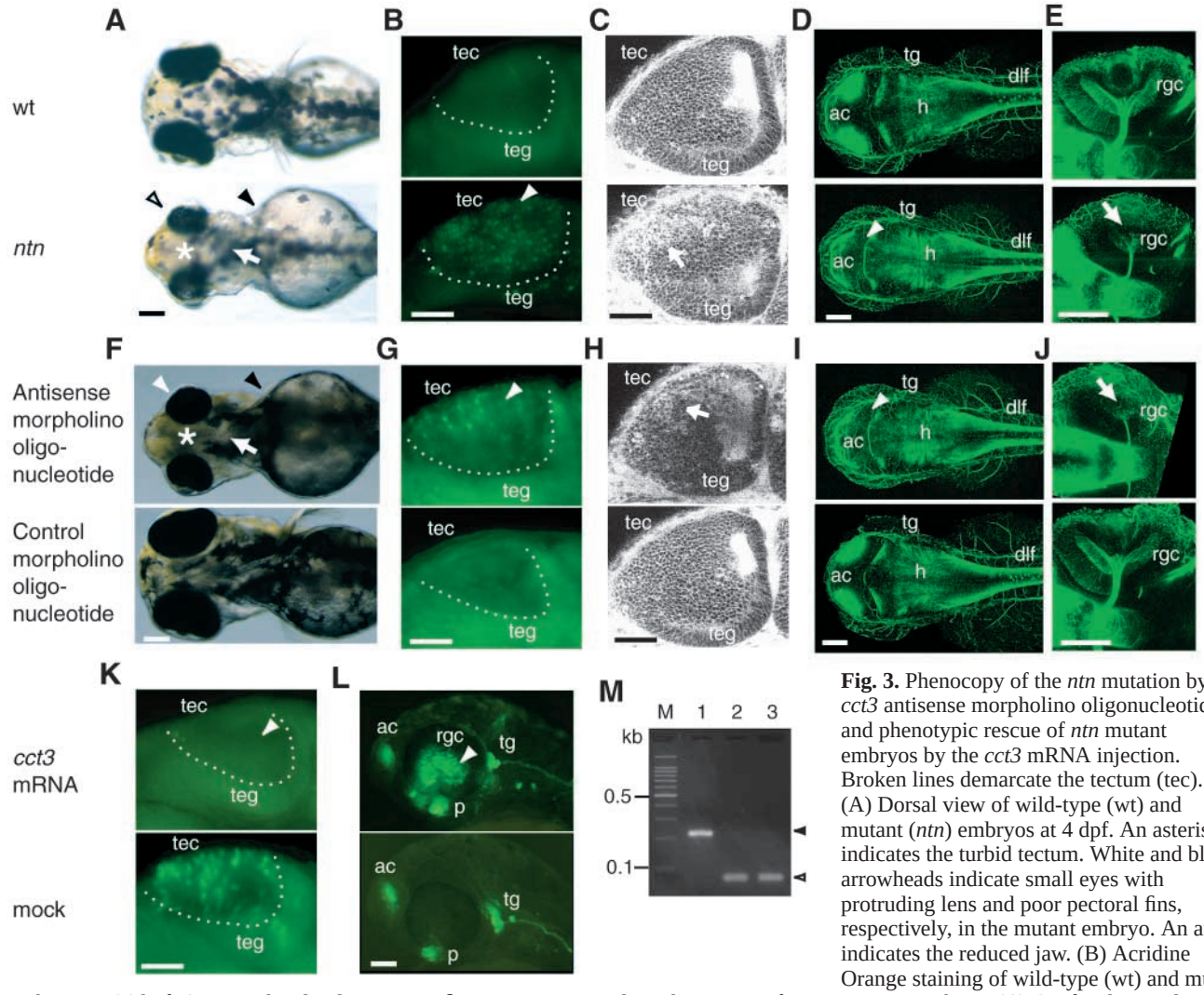

Fig. 3. Phenocopy of the *ntn* mutation by a *cct3* antisense morpholino oligonucleotide and phenotypic rescue of *ntn* mutant embryos by the *cct3* mRNA injection. Broken lines demarcate the tectum (tec). (A) Dorsal view of wild-type (wt) and mutant (*ntn*) embryos at 4 dpf. An asterisk indicates the turbid tectum. White and black arrowheads indicate small eyes with protruding lens and poor pectoral fins, respectively, in the mutant embryo. An arrow indicates the reduced jaw. (B) Acridine Orange staining of wild-type (wt) and mutant (*ntn*) embryos at 36 hpf. An arrowhead indicates significant staining signals in the tectum of an *ntn* mutant embryo. (C) Confocal optical section images of the tectum of Bodipy-ceramide-stained wild-type (wt) and mutant (*ntn*) embryos at 46 hpf. An arrow indicates patches of dead cells. (D) Confocal composite images of anti-acetylated tubulin immunostaining of wild-type (wt) and mutant (*ntn*) embryos at 48 hpf. An arrowhead indicates absence of staining signals in the tectum of the mutant embryo. (E) Confocal composite images of the retinae of anti-acetylated tubulin immunostained wild-type (wt) and mutant (*ntn*) embryos at 48 hpf. An arrow indicates decreased numbers of RGCs and their axons in the mutant embryo at 48 hpf. (F) Dorsal view of *cct3* antisense and control morpholino oligonucleotide-injected embryos at 4 dpf. White and black arrowheads indicate small eyes with protruding lens and poor pectoral fins, respectively, in the antisense-treated embryo. An asterisk indicates the turbid tectum. An arrow indicates the reduced jaw. (G) Acridine Orange staining of *cct3* antisense and control morpholino oligonucleotide-injected embryos at 36 hpf. An arrowhead indicates significant staining signals in the tectum of the antisense-treated embryo. (H) Confocal optical section images of the tectum of Bodipy-ceramide-stained *cct3* antisense and control morpholino oligonucleotide-injected embryos at 48 hpf. An arrow indicates patches of dead cells. (I) Confocal composite images of anti-acetylated tubulin immunostaining of *cct3* antisense and control morpholino oligonucleotide-injected embryos at 48 hpf. An arrowhead indicates the absence of staining signals in the tectum of the antisense-treated embryo. (J) Confocal composite images of the retinae of anti-acetylated tubulin immunostaining of *cct3* antisense and control morpholino oligonucleotide-injected embryos at 48 hpf. An arrow indicates decreased numbers of RGCs and their axons in the antisense-treated embryo at 48 hpf. (K) Acridine Orange staining of *cct3* mRNA- and mock-injected *ntn* embryos at 36 hpf. An arrowhead indicates the absence of staining signals in the tectum of the treated *ntn* embryo. (L) Expression of nAChRβ3 gene promoter-driven EGFP in *cct3* mRNA- and mock-injected *ntn* embryos at 48 hpf. An arrowhead indicates the recovery of fluorescent signals in RGCs of a *cct3* mRNA-injected *ntn* embryo. (M) Genotyping of a wild-type sibling (lane 1), *cct3* mRNA- (lane 2) and mock-injected (lane 3) *ntn* embryos using primers flanking the 143 bp deletion in the *cct3* gene. Lane M shows 100 bp DNA ladder as size markers. Black and white arrowheads on the right indicate the 221 bp and 78 bp PCR products representing the intact and deleted *cct3* genes, respectively. ac, anterior commissure neurons; dlf, dorsal longitudinal fasciculus; p, pituitary gland; rgc, retinal ganglion cells; teg, tegmentum; tg, trigeminal ganglion. Scale bars: 50 μm.

development of RGCs (Fig. 3L). In control mock-injected embryos, no EGFP signals appeared in the retina. Genotypes of *ntn* embryos injected with *cct3* mRNA showing wild-type phenotypes were confirmed to be $cct3^{-/-}$ at the *ntn* locus by PCR using the primers flanking the deletion in the *cct3* gene (Fig. 3M).

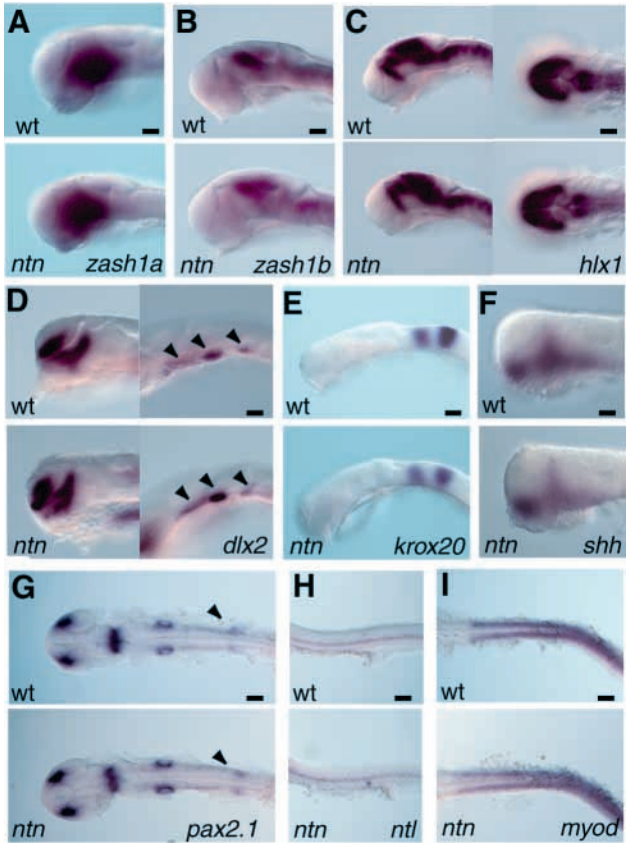

Fig. 4. Expression patterns of developmental landmark genes in wild-type (wt, upper panels) and *ntn* mutant (lower panels) embryos at 30 hpf. Lateral views of embryos stained by in situ hybridization with (A) antisense *zash1a* probe; (B) antisense *zash1b* probe; (C, left) antisense *hlx1* probe; (D) antisense *dlx2* probe; (E) antisense *krox20* probe; (F) antisense *shh* probe; (G) antisense *pax2a* probe; (H) antisense *ntl* probe. (I) antisense *myod* probe. (C, right) Dorsal view of embryo stained by in situ hybridization with antisense *hlx1* probe. Arrowheads in D indicate pharyngeal arches; arrowheads in G indicate pronephric ducts. Scale bars: 100 μm in A-D,F; 50 μm in E,G-I.

Impairment of retinotectal development in *ntn* mutant zebrafish

Chaperones play an important role in folding of many proteins and CCT is a member of two major chaperone systems implicated in cytoplasmic protein folding in eukaryotes (Bukau and Horwich, 1998; Hartl and Hayer-Hartl, 2002). By 12 hpf, the strong expression of the *cct3* mRNA started in entire zebrafish embryos and continued thereafter (Fig. 2D). In the segmentation period (10-24 hpf), a variety of morphogenetic movements occur: the somites develop, the rudiments of the primary organs become visible and the overall body length of the embryo increases very rapidly (Kimmel et al., 1995). Thus, we investigated whether there were any changes in body patterning or neurogenesis in *ntn* mutant embryos at 30 hpf. Two zebrafish homologs of the neurogenic gene *achaete-scute*, *zash1a* (*asha* – Zebrafish Information Network) and *zash1b*, were strongly expressed in the entire neural retina (Fig. 4A), and in the midbrain and hindbrain (Fig. 4B) of both wild-type and *ntn* embryos at 30 hpf, respectively. Between wild-type and *ntn* embryos, there were no differences in the expression patterns of the homeobox gene *hlx1* (*dbx1a* – Zebrafish Information Network) in the midbrain (Fig. 4C), *dlx2* in the telencephalon and diencephalon (Fig. 4D), *krox20* (*egr2b* – Zebrafish Information Network) in rhombomeres 3 and 5 (Fig. 4E), and *pax2a* in the midbrain-hindbrain boundary (Fig. 4G). The expression patterns of *dlx2* in the pharyngeal arches (Fig. 4D), *shh* in midline structures (Fig. 4F), *pax2a* in the optic stalk, otic vesicle and pronephric duct (Fig. 4G), *ntl* in the notochord (Fig. 4H) and *myod* in the myotomes (Fig. 4I) were also comparable between wild-type and mutant embryos. Thus, the development of zebrafish embryos appeared to have proceeded normally until 30 hpf without the CCTγ subunit.

To examine the role of the *cct3* gene more precisely, we analyzed retinotectal development in *ntn* mutant embryos by Bodipy-ceremide and TUNEL staining and by expression patterns of differentiation markers. Zebrafish neural retina consists of proliferating neuroepithelial cells at 27 hpf (Hu and Easter, 1999). The differentiation of RGCs began in the ventronasal region of the retina at 28 hpf, then increasingly spread over the central region of the retina until 37 hpf (Hu and Easter, 1999; Malicki, 1999; Schmitt and Dowling, 1999; Tokuoka et al., 2002). Bodipy-ceremide staining showed that retinal neuroepithelial cells with elongated shapes were arranged radially and expanding in both wild-type and mutant embryos at 27 hpf and 36 hpf (Fig. 5A). No differences were detectable in cellular morphology and alignment between wild-type and mutant retinae at these stages. At 48 hpf, the number of retinal cells increased and their radial alignment became less prominent in wild-type embryos (Fig. 5A). However, the staining revealed a loss of significant numbers of cells in the inner region of the retina in mutant embryos, although differentiation of the lens vesicle to the lens and onionskin organization of the lens proceeded normally. Consistent with the results of Bodipy-ceremide staining, there were no significant differences in TUNEL staining between wild-type and *ntn* mutant embryos at 30 hpf and 36 hpf (Fig. 5B). At 48 hpf, clusters of TUNEL-positive cells were found in the peripheral region of the mutant retina, suggesting the occurrence of apoptotic cell death. However, the ciliary marginal zone where neuroepithelial cells proliferated was TUNEL negative. These results suggest that the *ntn* mutation affected postmitotic developments rather than the proliferation of neuroepithelial cells.

RGCs are the first postmitotic neurons to be born in the zebrafish retina (Hu and Easter, 1999). We thus examined retinal development by immunostaining with monoclonal antibody zn5, an RGC differentiation marker (Trevarrow et al., 1990). The zn5 antibody staining showed strong signals in the central region of the wild-type retina at 48 hpf, whereas little staining was detectable in the *ntn* mutant retina, indicating the failure of RGC differentiation (Fig. 5C). Disturbance of retinal lamination was observed in mutant embryos at 72 hpf (data not shown). To further investigate the development of RGCs, we examined the expression of the nAChRβ3 gene, an early RGC differentiation marker (Matter-Sadzinski et al., 2001), by crossing *ntn* heterozygotes with transgenic zebrafish carrying the nAChRβ3 gene promoter-driven EGFP transgene (Tokuoka et al., 2002). In wild-type embryos, RGCs with EGFP signals appeared in the ventronasal region of the retina at 30 hpf, spread in the central region of the retina at 36 hpf and expanded

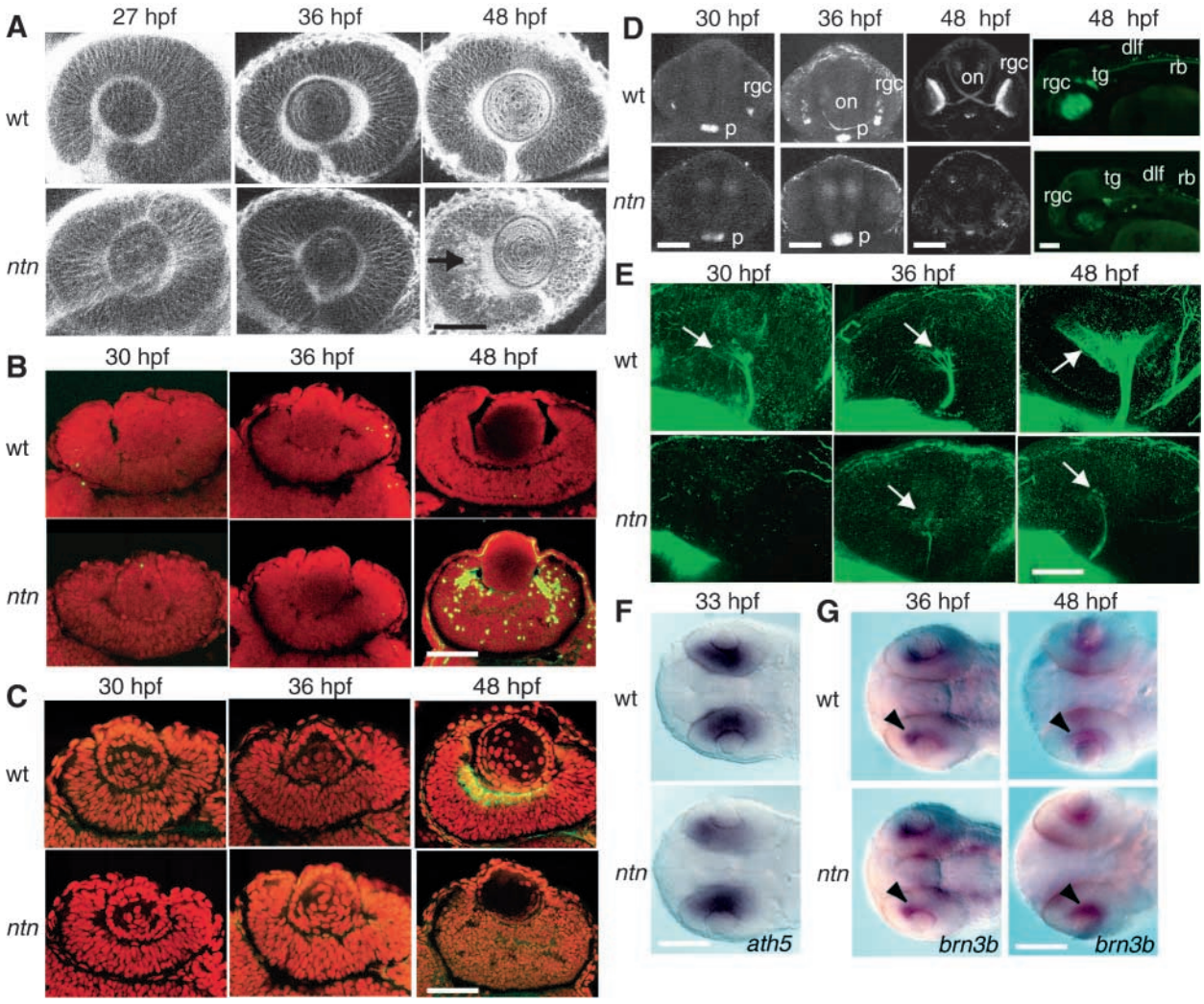

Fig. 5. Impairment of retinal development in *ntn* mutant embryos. (A) Confocal optical section images through the retina of Bodipy-ceramide stained wild-type (wt) and mutant (*ntn*) embryos at 27 hpf, 36 hpf and 48 hpf. An arrow indicates cell-free spaces. (B) TUNEL staining of retinal sections of wild-type (wt) and mutant (*ntn*) embryos at 30 hpf, 36 hpf and 48 hpf. (C) Immunostaining with zn5 antibody (green) of retinal sections of wild-type (wt) and mutant (*ntn*) embryos at 30 hpf, 36 hpf and 48 hpf. Nuclei of retinal cells were counterstained with Sytox (red). (D) Confocal composite images of nAChRβ3 gene promoter-driven EGFP signals in wild-type (wt) and mutant (*ntn*) embryos at 30 hpf, 36 hpf and 48 hpf in coronal view and those at 48 hpf in lateral view. Wild-type embryos have RGCs over the entire retina, whereas *ntn* mutants have sparse RGCs. Note that *ntn* mutants show EGFP signals in the trigeminal ganglion and Rohon-Beard sensory neurons and the pituitary gland. dlf, dorsal longitudinal fasciculus; on, optic nerve; p, pituitary gland; rb, Rohon-Beard neurons; tg, trigeminal ganglion. (E) Confocal composite images of immunostaining with anti-acetylated tubulin of retinal sections of wild-type (wt) and mutant (*ntn*) embryos at 30 hpf, 36 hpf and 48 hpf. Arrows indicate RGC axons. (F) In situ hybridization of *ath5* mRNA in wild-type (wt) and mutant (*ntn*) embryos at 33 hpf. Ventral view. (G) In situ hybridization of *brn3b* mRNA in wild-type (wt) and mutant (*ntn*) embryos at 36 hpf and 48 hpf. Ventral view. Arrowheads indicate the RGC layer. Scale bars: 50 μm in A-C; 100 μm in D-G.

in the inner retina to form the ganglion cell layer at 48 hpf (Fig. 5D). Retinal axons crossed the midline at 36 hpf and were extending towards the tectum at 48 hpf. In the mutant embryos, however, little EGFP signal was detectable in RGCs at 30 hpf, 36 hpf and 48 hpf (Fig. 5D). By contrast, EGFP signals in the trigeminal ganglion cells, Rohon-Beard sensory neurons and pituitary gland of mutant embryos were as strong as those of the wild-type embryos. The dorsal longitudinal fascicles and the axon fasciculation of trigeminal ganglion cells were comparable between wild-type and mutant embryos. Immunostaining with antibodies against acetylated tubulin, a general differentiation marker of neurons (Chitnis and Kuwada, 1990), showed that a small number of RGCs in the central region of the wild-type retina extended their axons at 30 hpf and 36 hpf (Fig. 5E). Anti-acetylated tubulin antibody stained RGC axons expanded in the inner retina and formed thick bundles at 48 hpf. However, little immunoreactivity to acetylated tubulin was detectable in the central region of the *ntn* mutant retina. At 36 hpf and 48 hpf, there were faint signals in the central region of the mutant retina, indicating poor development of RGCs. We next examined the expression of the proneural basic helix-loop-helix transcription factor atonal homolog 5 (*ath5/lakritz*; *atoh7* – Zebrafish Information Network) as a marker for retinal neurogenesis by in situ

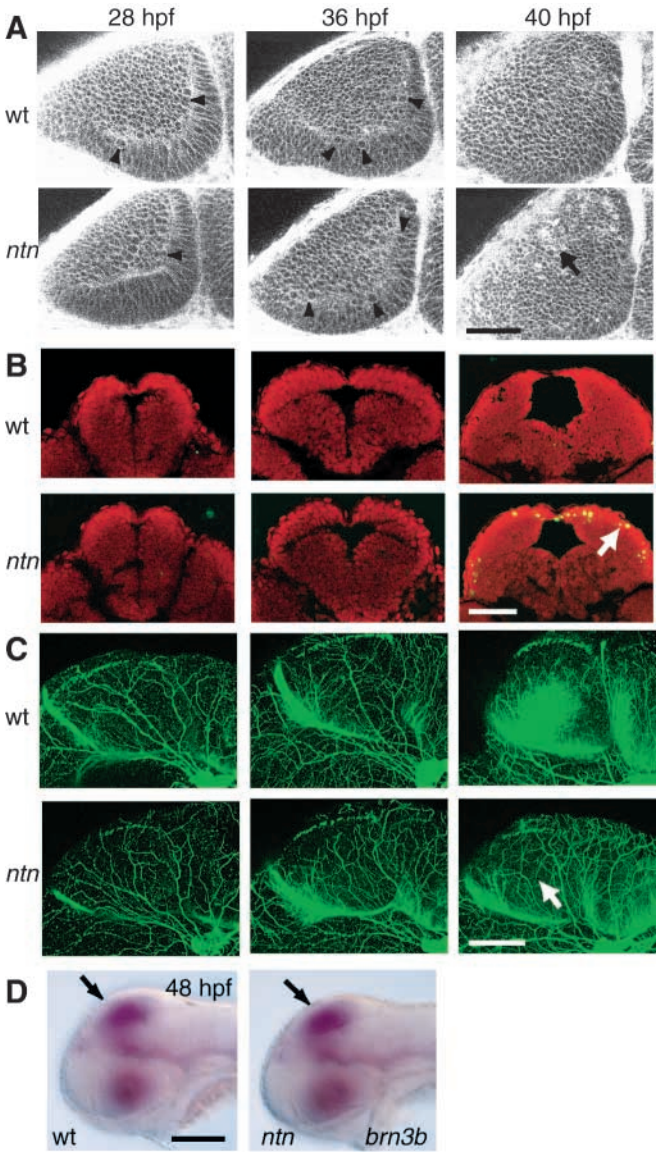

Fig. 6. Impairment of tectal development in *ntn* mutant embryos. (A) Confocal optical section images of the tectum of Bodipy-ceramide stained wild-type (wt) and mutant (*ntn*) embryos at 28 hpf, 36 hpf and 40 hpf. An arrow indicates cell-free spaces. Arrowheads point large and round cells representing mitotically active cells. (B) TUNEL staining of coronal sections through the tectum of wild-type (wt) and mutant (*ntn*) embryos at 30 hpf, 36 hpf and 40 hpf. An arrow indicates TUNEL-positive cells. (C) Confocal composite images of immunostaining with anti-acetylated tubulin antibody of wild-type (wt) and mutant (*ntn*) embryos at 30 hpf, 36 hpf and 40 hpf. An arrow indicates the absence of tectal neuropil. (D) In situ hybridization of *brn3b* mRNA in wild-type (wt) and mutant (*ntn*) embryos at 48 hpf. Dorsolateral view. Arrows indicate the tectum. Scale bars: 50 μm in A,C; 100 μm in B,D.

hybridization. The expression pattern of *ath5* in the retina was comparable between wild-type and mutant embryos at 33 hpf (Fig. 5F). Furthermore, a zebrafish homolog of the POU transcription factor *brn3b* (*pou4f1* – Zebrafish Information Network), a gene essential for the differentiation of RGCs (Xiang, 1998), showed similar expression patterns in the wild-type and mutant retinae at 36 hpf and 48 hpf (Fig. 5G). These results suggest that *ntn* mutation of the *cct3* gene exerted little effect on the commitment of retinal neuroepithelial cells to postmitotic retinal neurons but severely impaired the differentiation of retinal neuroepithelial cells to RGCs. Apoptosis of retinal cells observed after the impairment of RGC differentiation may be secondary effects of the *ntn* mutation.

We also analyzed the development of tectal neurons by staining with Bodipy-ceremide (Fig. 6A). Zebrafish tectal cells proliferated over the whole extent of the tectal plate at 24 hpf and many tectal precursor cells turned into postmitotic cells forming the central differentiated zone by 48 hpf, while cells in the peripheral marginal zone still remained proliferative (Wullimann and Knipp, 2000). Large and round cells representing mitotically active cells (Cooper et al., 1999) were found along the edge of the tectum in wild-type embryos at 28 hpf and 36 hpf. During development from 28 hpf to 36 hpf, the total volume of the tectum remained relatively constant, whereas each tectal neuron precursor became smaller in wild-type embryos. The ventricle between the tectum and the posterior tectal membrane became less prominent in wild-type embryos from 36 hpf to 40 hpf. There were no detectable abnormalities in the organization of the tectal neuroepithelium, alignment and mitotic cell images of tectal precursor neurons in *ntn* embryos at 28 hpf and 36 hpf. At 40 hpf, however, staining revealed cell-free spaces in the central zone of the tectum in mutant embryos. Consistently, TUNEL staining signals appeared in the tectum of mutant embryos at 40 hpf, but not at 30 hpf and 36 hpf (Fig. 6B). Immunostaining with anti-acetylated tubulin visualized the axons of trigeminal ganglion cells extending along the epidermis over the tectum and there were no significant differences in the immunostaining patterns of the tectum between wild-type and mutant embryos at 30 hpf and 36 hpf (Fig. 6C). At 40 hpf, immunostaining showed the formation of tectal neuropil by vigorous neurite extension of tectal neurons in wild-type embryos, but there was little staining in mutant embryos. However, the expression pattern of *brn3b* in tectal cells was comparable between wild-type and mutant embryos at 48 hpf (Fig. 6D), indicating the presence of tectal neurons. These results suggest that the *ntn* mutation of the *cct3* gene exerted little effect on the production of tectal cells but suppressed their differentiation to form tectal neuropil.

Discussion

TMP mutagenesis and RDA cloning

We developed TMP mutagenesis procedures in zebrafish in an attempt to facilitate the cloning of the mutated genes (Ando and Mishina, 1998). TMP, in combination with UV irradiation, forms interstrand crosslinks with DNA double helices and frequently results in deletions, possibly via incomplete nucleotide excision and recombination repair in *E. coli* and *C. elegans* (Cimino et al., 1985; Sladek et al., 1989; Yandell et al., 1994). Subtraction of the mutant genome from the wild-type genome should yield deleted genes or tightly linked RFLP markers. The ability to directly clone the mutated gene by the whole-genome subtraction method of Lisitsyn and Wigler (Lisitsyn and Wigler, 1993) crucially depends upon the size of a deletion and the presence of two restriction enzyme sites

within the deleted segment. Because the sizes of deletions were 0.1 to 15 kb in *C. elegans* (Yandell et al., 1994; Jansen et al., 1997; Liu et al., 1999), we selected five restriction enzymes suitable for PCR-based amplicon preparations from zebrafish genomic DNA to increase the probability of success. Three to four rounds of subtraction between *ntn* and wild-type littermate genomes digested with respective restriction enzymes yielded one to six RDA products. We thus successfully isolated polymorphic markers tightly linked to the *ntn* locus, although none of the RDA products was deleted in the mutant genome. These markers enabled us to obtain YAC clones carrying the *ntn* locus and to identify a deletion in the chaperonin *cct3* gene as the cause of *ntn* mutation.

Our results demonstrate that the combination of TMP mutagenesis and genetically directed RDA provides a highly efficient and rapid cloning strategy for zebrafish forward genetics. Using RDA products from a TMP-induced zebrafish mutant, *vibrato*, with defects in the spontaneous contraction and touch response, we also successfully constructed a high-resolution physical map of a genomic region of 720 kb containing the mutant locus (Sato and Mishina, 2003). The whole-genome subtraction method will be also applicable to zebrafish mutants induced by ENU. In addition to the 143 bp deletion in the *cct3* gene, there were two small deletions in ~5 kb *ntn* genomic region, indicating successful TMP deletion mutagenesis in zebrafish. We also found larger deletions in the genome of *edawakare*^{jt10} mutant zebrafish obtained by TMP mutagenesis (T. Morita, unpublished). Thus, direct selection by RDA of the mutated genes from TMP-induced mutant fish would be feasible depending on the sizes of deletions induced. In *C. elegans*, deletion sizes were dependent on TMP concentrations (Gengyo-Ando and Mitani, 2000).

Chaperonin CCTγ is essential for retinotectal development

In the present investigation, we identified the γ subunit of chaperonin CCT as an essential regulator of retinotectal development in zebrafish by whole-genome subtraction cloning from TMP-induced *ntn* mutants. Induction of *ntn* phenotypes by injection of *cct3* antisense morpholino oligonucleotide into wild-type embryos and rescue of *ntn* mutants by injection of wild-type *cct3* mRNA clearly showed that the impaired retinotectal development in the *ntn* mutant fish was caused by the mutation in the chaperonin *cct3* gene. The *ntn*^{jt5} mutation appears to be null because the deletion causes frameshift of translation. Available information suggests the presence of a single gene for the CCTγ subunit as well as the α, δ, ε, ζ, η and θ subunits in the zebrafish genome (http://www.ensembl.org/Danio_rerio/). A *cct3* zebrafish mutant was on the list of retroviral insertion mutants but no characterization was reported (Golling et al., 2002).

Molecular chaperones play an important role in folding of many proteins and CCT is a member of two major chaperone systems implied in cytoplasmic protein folding in eukaryotes (Bukau and Horwich, 1998; Hartl and Hayer-Hartl, 2002). In mammalian cells, ~15-20% of newly synthesized proteins transiently bind to Hsp70 and ~9-15% of them interact with CCT (Thulasiraman et al., 1999). Pharmacological inhibition of Hsp90, which cooperates with Hsp70 in folding of signal-transduction proteins (Young et al., 2001), was lethal and affected the development of various organs in zebrafish embryos (Lele et al., 1999). In addition, compromised Hsp90 activity in *Drosophila* and *Arabidopsis* caused a wide array of morphological variations, suggesting that Hsp90 acts as a capacitor for evolution (Rutherford and Landquist, 1998; Queitsh et al., 2002). Thus, it is surprising that the impairment of CCTγ caused defects specifically in coordinate retinotectal development of zebrafish. The causal relationship between CCTγ defect and the degeneration of retinal and tectal cells implies the importance of chaperones in neurodegenerative diseases (Slavotinek and Biesecker, 2001). CCT is a large cylindrical complex composed of eight different subunits providing physically defined compartments inside which a complete protein or a protein domain can fold while being sequestered from the cytosol (Kubota et al., 1995; Llorca et al., 1999). It is possible that the defect of the γ subunit in *ntn* mutants can be compensated by other CCT subunits to form functional CCT complex that assist folding of many proteins except for those specifically dependent on the γ subunit. The finding that the binding of actin to CCT is both subunit specific and geometry dependent (Vinh and Drubin, 1994; Llorca et al., 1999) may be consistent with this view. Major substrates of CCT are tubulin and actin in mammalian and yeast cells (Stoldt et al., 1996; Thulasiraman et al., 1999). In fact, CCT is essential for mitosis and growth in budding yeast *Saccharomyces cerevisiae* and conditional mutations in individual CCT subunit genes affect biogenesis of tubulin and/or actin (Chen et al., 1994; Stoldt et al., 1996). However, there was no detectable expression of the *cct3* mRNA in zebrafish embryos from one-cell to 90%-epiboly stages when vigorous cell proliferation and gastrulation took place. The *cct3* mRNA was strongly expressed at 12 hpf in the entire embryo and sustained thereafter, but the defects in development of *ntn* mutant embryos became detectable only at ~30 hpf and specifically in the retinotectal system. Anti-acetylated tubulin immunostaining in most of neurons other than RGCs and tectal neuropil was comparable between wild-type and *ntn* mutant embryos. It is known that axonogenesis also involves actin biogenesis and polymerization (Chien et al., 1993). Thus, it is unlikely that the *ntn* mutation directly impaired the actin and/or tubulin biogenesis. Transducin α requires CCT activity for folding (Farr et al., 1993). However, unlike *ntn* mutants, zebrafish transducin α mutants showed morphologically normal retina (Brockerhoff et al., 2003).

ntn mutation impaired differentiation of retinal and tectal neurons

One may speculate that the effect of the *ntn* mutation of the CCTγ gene on the retinotectal development is rather nonspecific, as CCT complex should assist folding of many proteins and zebrafish mutants affecting both retina and tectum were frequently found in large-scale screens (Abdelilah et al., 1996; Furutani-Seiki et al., 1996). However, the specificity of the *ntn* phenotypes is threefold. First, there were no detectable abnormalities in body patterning and neurogenesis in *ntn* mutant embryos at 30 hpf, despite the fact that the strong expression of the *cct3* mRNA in the entire embryos started by 12 hpf and that very active developmental changes occurred in the segmentation period (10-24 hpf), including a variety of morphogentic movements, the development of somites and primary organ rudiments and rapid increase in overall body length of the embryo (Kimmel et al., 1995). Second, *ntn*

phenotypes appeared specifically in the retina and tectum at ~2 dpf. At later stages (4 dpf), however, underdevelopment of pectoral fins and some jaw skeletons were noted in addition to small eyes and turbid tectum. Such abnormalities may be caused secondarily or may represent nonspecific effects. Third, a specific step in RGC differentiation is impaired in *ntn* mutants. The cellular organization of the retinal neuroepithelium at 27 and 36 hpf suggested that the formation of eye primordium, the proliferation of retinal cell progenitors and retinal patterning proceeded normally in *ntn* mutant embryos. The expression patterns of transcription factors *ath5* and *brn3b*, which are essential for the development and maintenance of RGCs (Erkman et al., 1996; Xiang, 1998; Brown et al., 2001; Kay et al., 2001; Matter-Sadzinski et al., 2001), were indistinguishable between wild-type and *ntn* mutant embryos, but those of early and late differentiation markers of RGCs, nAChRβ3 and zn5, were diminished in mutant embryos. Immunostaining of acetylated tubulin also revealed the impairment of RGC axon extension and optic nerve formation. Thus, *ntn* mutation of the *cct3* gene exerted little effect on the commitment of retinal neuroepithelial cells to postmitotic retinal neurons but severely impaired the differentiation of retinal neuroepithelial cells to RGCs. Similarly, the expression of *brn3b* was normal in the tectum of *ntn* mutants, but tectal neuropil formation was abolished. These results suggest that the γ subunit of chaperonin CCT plays an essential role in retinotectal development.

We are grateful to T. Morita and T. Sato for helpful advice on RDA procedures; I. Masai and M. Take-uchi for advice on the analysis of retinal development; T. Kaneko and S. Fukuoka for technical assistance; and K. Kinomoto for help in zebrafish breeding. We thank A. Chitnis for *dlx2* cDNA; T. Jowett for *krox20* cDNA; S. Krauss for *shh* cDNA; I. Masai for *ath5* cDNA; S. Shulte-Merker for *ntl* cDNA; H. Takeda for *hlx1*, *myod* and *pax2a* cDNAs; and E. Weinberg for *zash1a* and *zash1b* cDNAs. We also thank H. Mori and T. Yoshida for critical reading of the manuscript. We are grateful to M. Ohtsuka for his encouragement and support. This work was supported in part by research grants from the Japan Science and Technology Agency and the Ministry of Education, Culture, Sports, Science and Technology of Japan.

References

Abdelilah, S., Mountcastle-Shah, E., Harvey, M., Solnica-Krezel, L., Schier, A. F., Stemple, D. L., Malicki, J., Neuhauss, S. C., Zwartkruis, F., Stainier, D. Y. et al. (1996). Mutations affecting neural survival in the zebrafish *Danio rerio*. *Development* **123**, 217-227.

Abrams, J. M., White, K., Fessler, L. I. and Steller, H. (1993). Programmed cell death during *Drosophila* embryogenesis. *Development* **117**, 29-43.

Akimenko, M. A., Ekker, M., Wegner, J., Lin, W. and Westerfield, M. (1994). Combinatorial expression of three zebrafish genes related to *distal-less*: part of a homeobox gene code for the head. *J. Neurosci.* **14**, 3475-3486.

Allende, M. L. and Weinberg, E. S. (1994). The expression pattern of two zebrafish *achaete-scute homolog* (*ash*) genes is altered in the embryonic brain of the cyclops mutant. *Dev. Biol.* **166**, 509-530.

Amsterdam, A., Burgess, S., Golling, G., Chen, W., Sun, Z., Townsend, K., Farrington, S., Haldi, M. and Hopkins, N. (1999). A large-scale insertional mutagenesis screen in zebrafish. *Genes Dev.* **13**, 2713-2724.

Ando, H. and Mishina, M. (1998). Efficient mutagenesis of zebrafish by a DNA cross-linking agent. *Neurosci. Lett.* **244**, 81-84.

Brockerhoff, S. E., Rieke, F., Matthews, H. R., Taylor, M. R., Kennedy, B., Ankoudinova, I., Niemi, G. A., Tucker, C. L., Xiao, M., Cilluffo, M. C. et al. (2003). Light stimulates a transducin-independent increase of cytoplasmic Ca^{2+} and suppression of current in cones from the zebrafish mutant *nof*. *J. Neurosci.* **23**, 470-480.

Brown, N. L., Patel, S., Brzezinski, J. and Glaser, T. (2001). Math5 is required for retinal ganglion cell and optic nerve formation. *Development* **128**, 2497-2508.

Bukau, B. and Horwich, A. L. (1998). The Hsp70 and Hsp60 chaperone machines. *Cell* **92**, 351-366.

Chen, X., Sullivan, D. S. and Huffaker, T. C. (1994). Two yeast genes with similarity to TCP-1 are required for microtubule and actin function in vivo. *Proc. Natl. Acad. Sci. USA* **91**, 9111-9115.

Chien, C. B., Rosenthal, D. E., Harris, W. A. and Holt, C. E. (1993). Navigational errors made by growth cones without filopodia in the embryonic *Xenopus* brain. *Neuron* **11**, 237-251.

Chitnis, A. B. and Kuwada, J. Y. (1990). Axonogenesis in the brain of zebrafish embryos. *J. Neurosci.* **10**, 1892-1905.

Cimino, G. D., Gamper, H. B., Isaacs, S. T. and Hearst, J. E. (1985). Psoralens as photoactive probes of nucleic acid structure and function: organic chemistry, photochemistry, and biochemistry. *Annu. Rev. Biochem.* **54**, 1151-1193.

Cooper, M. S., D'Amico, L. A. and Henry, C. A. (1999). Confocal microscopic analysis of morphogenetic movements. *Methods Cell Biol.* **59**, 179-204.

Del Mastro, R. G. and Lovett, M. (1996). Isolation of coding sequences from genomic regions using direct selection. In *Methods in Molecular Biology*, Vol. 68 (ed. J. Bolultwood), pp. 183-199. Totowa, NJ: Humana Press.

Driever, W., Solnica-Krezel, L., Schier, A. F., Neuhauss, S. C., Malicki, J., Stemple, D. L., Stainier, D. Y., Zwartkruis, F., Abdelilah, S., Rangini, Z. et al. (1996). A genetic screen for mutations affecting embryogenesis in zebrafish. *Development* **123**, 37-46.

Dunn, M. K. and Mercola, M. (1996). Cloning and expression of *Xenopus* CCTγ, a chaperonin subunit developmentally regulated in neural-derived and myogenic lineages. *Dev. Dyn.* **205**, 387-394.

Easter, S. S., Jr and Nicola, G. N. (1996). The development of vision in the zebrafish (*Danio rerio*). *Dev. Biol.* **180**, 646-663.

Eisen, J. S. (1996). Zebrafish make a big splash. *Cell* **87**, 969-977.

Erkman, L., McEvilly, R. J., Luo, L., Ryan, A. K., Hooshmand, F., O'Connell, S. M., Keithley, E. M., Rapaport, D. H., Ryan, A. F. and Rosenfeld, M. G. (1996). Role of transcription factors Brn-3.1 and Brn-3.2 in auditory and visual system development. *Nature* **381**, 603-606.

Farr, G. W., Scharl, E. C., Schumacher, R. J., Sondek, S. and Horwich, A. L. (1997). Chaperonin-mediated folding in the eukaryotic cytosol proceeds through rounds of release of native and nonnative forms. *Cell* **89**, 927-937.

Furutani-Seiki, M., Jiang, Y. J., Brand, M., Heisenberg, C. P., Houart, C., Beuchle, D., van Eeden, F. J., Granato, M., Haffter, P., Hammerschmidt, M. et al. (1996). Neural degeneration mutants in the zebrafish, *Danio rerio*. *Development* **123**, 229-239.

Gaiano, N., Amsterdam, A., Kawakami, K., Allende, M., Becker, T. and Hopkins, N. (1996). Insertional mutagenesis and rapid cloning of essential genes in zebrafish. *Nature* **383**, 829-832.

Geisler, R., Rauch, G. J., Baier, H., van Bebber, F., Brobeta, L., Dekens, M. P., Finger, K., Fricke, C., Gates, M. A., Geiger, H. et al. (1999). A radiation hybrid map of the zebrafish genome. *Nat. Genet.* **23**, 86-89.

Gengyo-Ando, K. and Mitani, S. (2000). Characterization of mutations induced by ethyl methanesulfonate, UV, and trimethylpsoralen in the nematode *Caenorhabditis elegans*. *Biochem. Biophys. Res. Commun.* **269**, 64-69.

Golling, G., Amsterdam, A., Sun, Z., Antonelli, M., Maldonado, E., Chen, W., Burgess, S., Haldi, M., Artzt, K., Farrington, S. et al. (2002). Insertional mutagenesis in zebrafish rapidly identifies genes essential for early vertebrate development. *Nat. Genet.* **31**, 135-140.

Haffter, P., Granato, M., Brand, M., Mullins, M. C., Hammerschmidt, M., Kane, D. A., Odenthal, J., van Eeden, F. J., Jiang, Y. J., Heisenberg, C. P. et al. (1996). The identification of genes with unique and essential functions in the development of the zebrafish, *Danio rerio*. *Development* **123**, 1-36.

Hammerschmidt, M., Pelegri, F., Mullins, M. C., Kane, D. A., van Eeden, F. J., Granato, M., Brand, M., Furutani-Seiki, M., Haffter, P., Heisenberg, C. P. et al. (1996). *dino* and *mercedes*, two genes regulating dorsal development in the zebrafish embryo. *Development* **123**, 95-102.

Hartl, F. U. and Hayer-Hartl, M. (2002). Molecular chaperones in the cytosol: from nascent chain to folded protein. *Science* **295**, 1852-1858.

Hu, M. and Easter, S. S. (1999). Retinal neurogenesis: the formation of the initial central patch of postmitotic cells. *Dev. Biol.* **207**, 309-321.

Jansen, G., Hazendonk, E., Thijssen, K. L. and Plasterk, R. H. (1997).

Reverse genetics by chemical mutagenesis in *Caenorhabditis elegans*. *Nat. Genet.* **17**, 119-121.

Jowett, T. (1999). Analysis of protein and gene expression. *Methods Cell Biol.* **59**, 63-85.

Kay, J. N., Finger-Baier, K. C., Roeser, T., Staub, W. and Baier, H. (2001). Retinal ganglion cell genesis requires *lakritz*, a zebrafish *atonal* homolog. *Neuron* **30**, 725-736.

Kikuchi, K., Chedotal, A., Hanafusa, H., Ujimasa, Y., de Castro, F., Goodman, C. S. and Kimura, T. (1999). Cloning and characterization of a novel class VI semaphorin, semaphorin Y. *Mol. Cell. Neurosci.* **13**, 9-23.

Kim, S., Willison, K. R. and Horwich, A. L. (1994). Cytosolic chaperonin subunits have a conserved ATPase domain but diverged polypeptide-binding domains. *Trends Biochem. Sci.* **19**, 543-548.

Kimmel, C. B., Ballard, W. W., Kimmel, S. R., Ullmann, B. and Schilling, T. F. (1995). Stages of embryonic development of the zebrafish. *Dev. Dyn.* **203**, 253-310.

Krauss, S., Johansen, T., Korzh, V. and Fjose, A. (1991). Expression of the zebrafish paired box gene *pax[zf-b]* during early neurogenesis. *Development* **113**, 1193-1206.

Krauss, S., Concordet, J. P. and Ingham, P. W. (1993). A functionally conserved homolog of the *Drosophila* segment polarity gene *hh* is expressed in tissues with polarizing activity in zebrafish embryos. *Cell* **75**, 1431-1444.

Kubota, H., Hynes, G., Carne, A., Ashworth, A. and Willison, K. (1994). Identification of six Tcp-1-related genes encoding divergent subunits of the TCP-1-containing chaperonin. *Curr. Biol.* **4**, 89-99.

Kubota, H., Hynes, G. and Willison, K. (1995). The chaperonin containing t-complex polypeptide 1 (TCP-1). Multisubunit machinery assisting in protein folding and assembly in the eukaryotic cytosol. *Eur. J. Biochem.* **230**, 3-16.

Lele, Z., Hartson, S. D., Martin, C. C., Whitesell, L., Matts, R. L. and Krone, P. H. (1999). Disruption of zebrafish somite development by pharmacologic inhibition of Hsp90. *Dev. Biol.* **210**, 56-70.

Lisitsyn, N. and Wigler, M. (1993). Cloning the differences between two complex genomes. *Science* **259**, 946-951.

Lisitsyn, N. and Wigler, M. (1995). Representational difference analysis in detection of genetic lesions in cancer. *Methods Enzymol.* **254**, 291-304.

Lisitsyn, N. A., Segre, J. A., Kusumi, K., Lisitsyn, N. M., Nadeau, J. H., Frankel, W. N., Wigler, M. H. and Lander, E. S. (1994). Direct isolation of polymorphic markers linked to a trait by genetically directed representational difference analysis. *Nat. Genet.* **6**, 57-63.

Liu, L. X., Spoerke, J. M., Mulligan, E. L., Chen, J., Reardon, B., Westlund, B., Sun, L., Abel, K., Armstrong, B., Hardiman, G. et al. (1999). High-throughput isolation of *Caenorhabditis elegans* deletion mutants. *Genome Res.* **9**, 859-867.

Llorca, O., McCormack, E. A., Hynes, G., Grantham, J., Cordell, J., Carrascosa, J. L., Willison, K. R., Fernandez, J. J. and Valpuesta, J. M. (1999). Eukaryotic type II chaperonin CCT interacts with actin through specific subunits. *Nature* **402**, 693-696.

Malicki, J. (1999). Development of the retina. *Methods Cell Biol.* **59**, 273-299.

Masai, I., Stemple, D. L., Okamoto, H. and Wilson, S. W. (2000). Midline signals regulate retinal neurogenesis in zebrafish. *Neuron* **27**, 251-263.

Masai, I., Lele, Z., Yamaguchi, M., Komori, A., Nakata, A., Nishiwaki, Y., Wada, H., Tanaka, H., Nojima, Y., Hammerschmidt, M. et al. (2003). N-cadherin mediates retinal lamination, maintenance of forebrain compartments and patterning of retinal neurites. *Development* **130**, 2479-2494.

Matter-Sadzinski, L., Matter, J. M., Ong, M. T., Hernandez, J. and Ballivet, M. (2001). Specification of neurotransmitter receptor identity in developing retina: the chick ATH5 promoter integrates the positive and negative effects of several bHLH proteins. *Development* **128**, 217-231.

Mori, H., Miyazaki, Y., Morita, T., Nitta, H. and Mishina, M. (1994). Different spatio-temporal expressions of three *otx* homeoprotein transcripts during zebrafish embryogenesis. *Mol. Brain Res.* **27**, 221-231.

Mullins, M. C., Hammerschmidt, M., Haffter, P. and Nusslein-Volhard, C. (1994). Large-scale mutagenesis in the zebrafish: in search of genes controlling development in a vertebrate. *Curr. Biol.* **4**, 189-202.

Nasevicius, A. and Ekker, S. C. (2000). Effective targeted gene 'knockdown' in zebrafish. *Nat. Genet.* **26**, 216-220.

Oxtoby, E. and Jowett, T. (1993). Cloning of the zebrafish *krox-20* gene (*krx-20*) and its expression during hindbrain development. *Nucleic Acids Res.* **21**, 1087-1095.

Postlethwait, J. H. and Talbot, W. S. (1997). Zebrafish genomics: from mutants to genes. *Trends Genet.* **13**, 183-190.

Queitsch, C., Sangster, T. A. and Lindquist, S. (2002). Hsp90 as a capacitor of phenotypic variation. *Nature* **417**, 618-624.

Rutherford, S. L. and Lindquist, S. (1998). Hsp90 as a capacitor for morphological evolution. *Nature* **396**, 336-342.

Sato, T. and Mishina, M. (2003). Representational difference analysis, high-resolution physical mapping and transcript identification of the zebrafish genomic region for a motor behavior. *Genomics* **82**, 218-229.

Schmitt, E. A. and Dowling, J. E. (1999). Early retinal development in the zebrafish, *Danio rerio*: light and electron microscopic analyses. *J. Comp. Neurol.* **404**, 515-536.

Schulte-Merker, S., van Eeden, F. J., Halpern, M. E., Kimmel, C. B. and Nusslein-Volhard, C. (1994). *no tail (ntl)* is the zebrafish homologue of the mouse T (Brachyury) gene. *Development* **120**, 1009-1015.

Seo, H. C., Nilsen, F. and Fjose, A. (1999). Three structurally and functionally conserved Hlx genes in zebrafish. *Biochim. Biophys. Acta* **1489**, 323-335.

Sladek, F. M., Melian, A. and Howard-Flanders, P. (1989). Incision by UvrABC excinuclease is a step in the path to mutagenesis by psoralen crosslinks in Escherichia coli. *Proc. Natl. Acad. Sci. USA* **86**, 3982-3986.

Slavotinek, A. M. and Biesecker, L. G. (2001). Unfolding the role of chaperones and chaperonins in human disease. *Trends Genet.* **17**, 528-535.

Solnica-Krezel, L., Schier, A. F. and Driever, W. (1994). Efficient recovery of ENU-induced mutations from the zebrafish germline. *Genetics* **136**, 1401-1420.

Stoldt, V., Rademacher, F., Kehren, V., Ernst, J. F., Pearce, D. A. and Sherman, F. (1996). Review: the Cct eukaryotic chaperonin subunits of Saccharomyces cerevisiae and other yeasts. *Yeast* **12**, 523-529.

Thulasiraman, V., Yang, C. F. and Frydman, J. (1999). In vivo newly translated polypeptides are sequestered in a protected folding environment. *EMBO J.* **18**, 85-95.

Tokuoka, H., Yoshida, T., Matsuda, N. and Mishina, M. (2002). Regulation by glycogen synthase kinase-3β of the arborization field and maturation of retinotectal projection in zebrafish. *J. Neurosci.* **22**, 10324-10332.

Trevarrow, B., Marks, D. L. and Kimmel, C. B. (1990). Organization of hindbrain segments in the zebrafish embryo. *Neuron* **4**, 669-679.

Turner, D. L. and Weintraub, H. (1994). Expression of achaete-scute homolog 3 in *Xenopus* embryos converts ectodermal cells to a neural fate. *Genes Dev.* **8**, 1434-1447.

Vinh, D. B. and Drubin, D. G. (1994). A yeast TCP-1-like protein is required for actin function in vivo. *Proc. Natl. Acad. Sci. USA* **91**, 9116-9120.

Walkley, N. A. and Malik, A. N. (1996). Drosophila melanogaster P1 genomic clone DS05563 contains the chaperonin-encoding gene Cctγ. *Gene* **171**, 221-223.

Walkley, N. A., Demaine, A. G. and Malik, A. N. (1996a). Cloning, structure and mRNA expression of human Cctγ, which encodes the chaperonin subunit CCT γ. *Biochem. J.* **313**, 381-389.

Walkley, N. A., Page, R. A. and Malik, A. N. (1996b). Molecular characterisation of the *Xenopus laevis* chaperonin gene Cctγ. *Biochim. Biophys. Acta* **1309**, 25-30.

Weinberg, E. S., Allende, M. L., Kelly, C. S., Abdelhamid, A., Murakami, T., Andermann, P., Doerre, O. G., Grunwald, D. J. and Riggleman, B. (1996). Developmental regulation of zebrafish MyoD in wild-type, *no tail* and *spadetail* embryos. *Development* **122**, 271-280.

Westerfield, M. (1995). *The Zebrafish Book.* Oregon: University of Oregon Press.

Wullimann, M. F. and Knipp, S. (2000). Proliferation pattern changes in the zebrafish brain from embryonic through early postembryonic stages. *Anat. Embryol.* **202**, 385-400.

Xiang, M. (1998). Requirement for Brn-3b in early differentiation of postmitotic retinal ganglion cell precursors. *Dev. Biol.* **197**, 155-169.

Yandell, M. D., Edgar, L. G. and Wood, W. B. (1994). Trimethylpsoralen induces small deletion mutations in *Caenorhabditis elegans*. *Proc. Natl. Acad. Sci. USA* **91**, 1381-1385.

Yoshikawa, T., Sanders, A. R., Esterling, L. E. and Detera-Wadleigh, S. D. (1998). Multiple transcriptional variants and RNA editing in C18orf1, a novel gene with LDLRA and transmembrane domains on 18p11.2. *Genomics* **47**, 246-257.

Young, J. C., Moarefi, I. and Hartl, F. U. (2001). Hsp90: a specialized but essential protein-folding tool. *J. Cell Biol.* **154**, 267-273.

Zhong, T. P., Kaphingst, K., Akella, U., Haldi, M., Lander, E. S. and Fishman, M. C. (1998). Zebrafish genomic library in yeast artificial chromosomes. *Genomics* **48**, 136-138.